Accepted Manuscript

Targeting the entry region of Hsp90's ATP binding pocket with a novel 6,7-dihydrothieno[3,2-c]pyridin-5(4H)-yl amide

Ju Hui Jeong, Yong Jin Oh, Yunmee Lho, Sun You Park, Kwang-Hyeon Liu, Eunyoung Ha, Young Ho Seo

PII: S0223-5234(16)30900-X

DOI: 10.1016/j.ejmech.2016.10.038

Reference: EJMECH 9003

To appear in: *European Journal of Medicinal Chemistry*

Received Date: 20 July 2016

Revised Date: 16 October 2016

Accepted Date: 17 October 2016

Please cite this article as: J.H. Jeong, Y.J. Oh, Y. Lho, S.Y. Park, K.-H. Liu, E. Ha, Y.H. Seo, Targeting the entry region of Hsp90's ATP binding pocket with a novel 6,7-dihydrothieno[3,2-c]pyridin-5(4H)-yl amide, *European Journal of Medicinal Chemistry* (2016), doi: 10.1016/j.ejmech.2016.10.038.

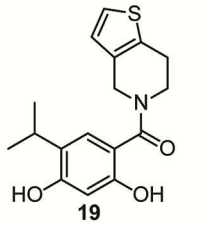

19

MW = 317

GI_{50} = 0.31 μM (H1975)
0.11 μM (Skbr3)

IC_{50} = 50.3 nM (Hsp90α)

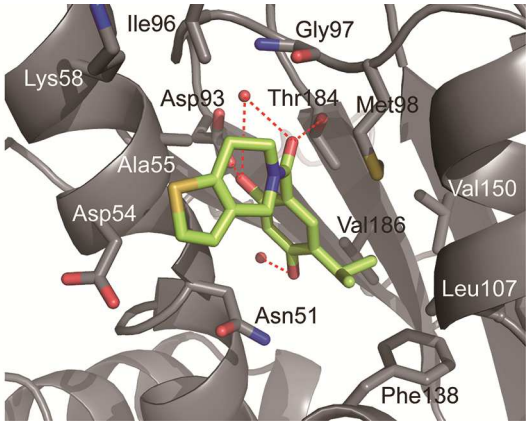

Title: Targeting the entry region of Hsp90′s ATP binding pocket with a novel 6,7-dihydrothieno[3,2-c]pyridin-5(4H)-yl amide

Ju Hui Jeong [a, 1], Yong Jin Oh [a, 1], Yunmee Lho [b], Sun You Park [a], Kwang-Hyeon Liu [c], Eunyoung Ha [b, **], Young Ho Seo [a, *]

[a] *College of Pharmacy, Keimyung University, Daegu 704-701, South Korea.*

[b] *Department of Biochemistry, School of Medicine, Keimyung University, Daegu 704-701, South Korea.*

[c] *BK21 Plus KNU Multi-Omics based Creative Drug Research Team, College of Pharmacy and Research Institute of Pharmaceutical Sciences, Kyungpook National University, Daegu 41566, South Korea.*

[*] Corresponding author

[**] Corresponding author

E-mail addresses: seoyho@kmu.ac.kr (Y. H. Seo), hanne.md@gmail.com (E. Ha)

[1] Authors are equal contributors

Graphical Abstract

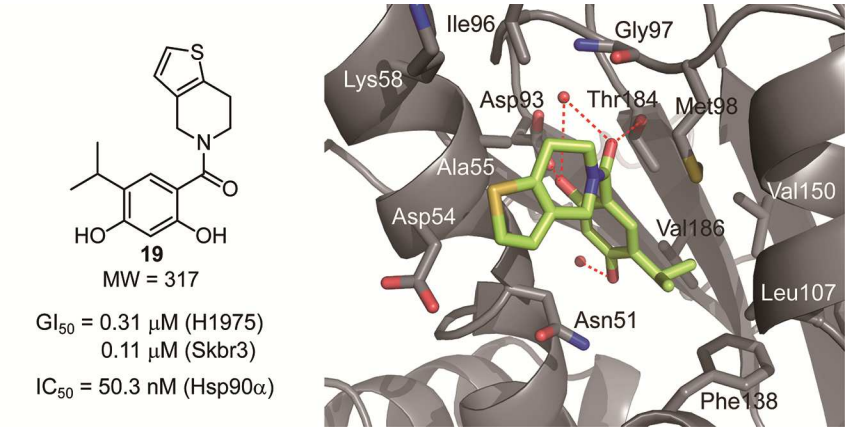

Highlights

- Design, synthesis, and biological evaluation of a series of Hsp90 inhibitors are presented.
- Compound **19** exhibits a remarkable anticancer activity against H1975 non-small cell lung cancer and Skbr3 breast cancer cell lines.
- Compound **19** inhibits the growth of H1975 xenografts in NOD-scid IL2Rgamma^{null} mice through Hsp90 inhibition.
- Compound **19** has no effect on the activities of five major P450 isoforms (IC_{50} > 50 μM for 1A2, 2C9, 2C19, 2D6, and 3A), suggesting that clinical interactions between compound **19** and the substrate drugs of the five major P450 isoforms are not expected.

Abstract

The molecular chaperone Hsp90 plays an important role in cancer cell survival and proliferation by regulating the maturation and stabilization of numerous oncogenic proteins. Due to its potential to simultaneously disable multiple signaling pathways, Hsp90 has emerged as an attractive therapeutic target for cancer treatment. In this study, the design, synthesis, and biological evaluation of a series of Hsp90 inhibitors are described. Among the synthetic compounds, 6,7-dihydrothieno[3,2-c]pyridin-5(4H)-yl amide **19** exhibits a remarkable binding affinity to the *N*-terminus of Hsp90 in a fluorescence polarization (FP) binding assay (IC_{50} = 50.3 nM). Furthermore, it effectively inhibits the proliferation of H1975 non-small cell lung cancer (NSCLC) and Skbr3 breast cancer cell lines with GI_{50} values of 0.31 μM and 0.11 μM, respectively. Compound **19** induces the degradation of the Hsp90 client proteins including EGFR, Her2, Met, c-Raf, and Akt, and consequently promotes apoptotic cancer cell death. Compound **19** also inhibits the growth of H1975 xenografts in NOD-scid IL2R gamma^{null} mice without any apparent body-weight loss. The immunohistologic evaluation indicates that compound **19** decreases the expression of Akt in xenograft tumor tissue via an inhibition of the Hsp90 chaperon function. Additionally, the cytochrome P450 assay indicates that compound **19** has no effect on the activities of five major P450 isoforms (IC_{50} > 50 μM for 1A2, 2C9, 2C19, 2D6, and 3A), suggesting that clinical interactions between compound **19** and the substrate drugs of the five major P450 isoforms are not expected. Overall, compound **19** represents a new class of Hsp90 inhibitor with its 6,7-dihydrothieno[3,2-c]pyridin-5(4H)-yl-amide structure, and it has the therapeutic potential to overcome drug resistance in cancer chemotherapy.

1. Introduction

Heat shock protein 90 (Hsp90) is an ATP-dependent molecular chaperone that is responsible for the correct folding, stability and function of its substrate proteins, referred to as “client” proteins. Many Hsp90 client proteins are oncogenic proteins that are involved in malignant behavior and cancer progression [1,2]. These client proteins include epidermal growth factor receptor (EGFR/ErbB1), human epidermal growth factor receptor 2 (Her2/ErbB2), mesenchymal-epithelial transition factor (Met), anaplastic lymphoma kinase (Alk), protein kinase B (Akt/PKB), cellular rapidly accelerated fibrosarcoma (c-Raf), cyclin-dependent kinase 4 (Cdk4), hypoxia-inducible factor 1 (Hif-1α), matrix metalloproteinase 2 (MMP2), mutant P53, and wee1 [3]. Due to the hostile environmental factors of cancer such as hypoxia, low pH, and poor nutrition, cancer cells depend more on the chaperone function of Hsp90 than normal cells, which explains 2-10 fold higher expression level of Hsp90 in cancer cells than normal cells [3-5]. Accordingly, the inhibition of Hsp90 chaperone function induces the degradation of the client proteins via the ubiquitin-proteasome pathway, and subsequently results in a simultaneous disruption of the multiple signaling pathways in cancer. Hsp90 consists of the following four major homologs; Hsp90α, Hsp90β, 94-kDa glucose-regulated protein (Grp94), and TNF receptor-associated protein 1 (Trap1) [6,7]. Hsp90α is an inducible form that is overexpressed in many cancer cells, and Hsp90β is the constitutive form. Both Hsp90α and Hsp90β are mainly localized in the cytoplasm, while Grp94 and Trap1 reside in the endoplasmic reticulum and the mitochondria, respectively. Hsp90 has been extensively pursued as a promising target for overcoming drug resistance. The potential therapeutic benefits associated with Hsp90 modulation emphasize the importance of identifying novel Hsp90 inhibitors [8-11].

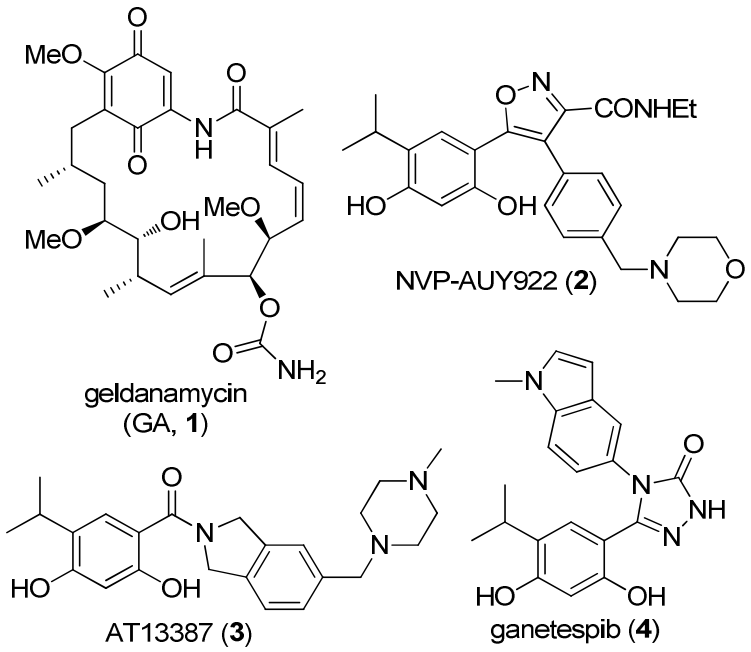

Figure 1. Structures of known Hsp90 inhibitors

Geldanamycin (GA, **1**), a benzoquinone ansamycin antibiotic was first identified as an Hsp90 inhibitor in 1994 [12]. Since then, a number of geldanamycin analogues such as tanespimycin (17-AAG) and alvespimycin (17-DMAG) have been developed and entered into clinical study [13]. However, these first-generation Hsp90 inhibitors engendered several drawbacks in the clinical applications such as a poor solubility and toxicity [14]. The most clinically significant toxicity of the geldanamycin analogues is liver toxicity. The liver toxicity was a major limitation in the clinical development, and it was speculated that the benzoquinone structure of geldanamycin analogues largely contribute to the observed liver toxicity [15].

Benefited from the X-ray crystal structures of Hsp90 and fragment-based drug discovery, investigators discovered the second-generation Hsp90 inhibitors, which are classified into two major cores, purine and resorcinol. The purine class of Hsp90 inhibitors are designed according to the structural homology of ATP and include PU-H71 [16], BIIB021 [17], and

CUDC-305 [18]. The resorcinol scaffold is another important class of Hsp90 inhibitors that includes NVP-AUY922 [19], KW-2478 [20], AT13387 [21] and STA-9090 [22]. Based on the wealth of compelling data from the preclinical studies, many of the second-generation Hsp90 inhibitors have entered into the clinical phase, and display an improved potency with a lesser liver toxicity [23]. Despite an enormous effort and promise, none of the Hsp90 inhibitors are clinically approved, and the full potential of this inhibitor clasee is yet to be realized. Accordingly, the discovery of Hsp90 inhibitors with different chemotypes is still a demanding task in this area.

2. Results and discussion

2.1. Analysis of ATP-binding site

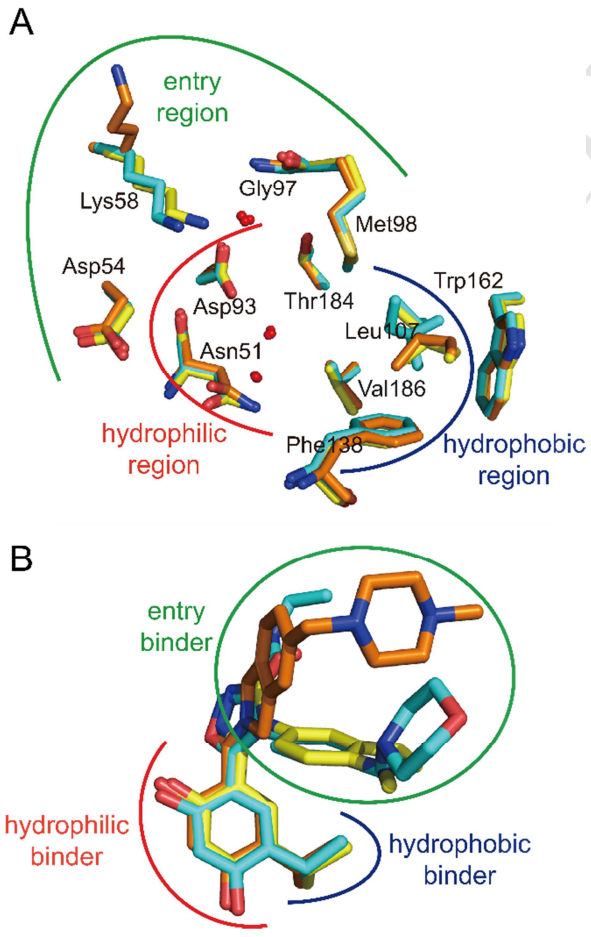

Figure 2. Analysis of ATP-binding site in the *N*-terminal domain of Hsp90 protein and the

binding poses of Hsp90 inhibitors in the ATP-binding site. (A) Superimposed crystal structures of three apo-Hsp90 proteins (PDB codes: 2XJX, orange; 2VCI, cyan; and 2TUH, yellow) and conserved waters (red-colored spheres), where the side chains of the binding site are colored by atom types (oxygen, red; nitrogen, blue). (B) Overlaid binding modes of AT13387 (orange), NVP-AUY922 (cyan), and STA-9090 (yellow) from co-crystal structures of Hsp90 (PDB codes: 2XJX, 2VCI, and 2TUH), where the oxygen and nitrogen atoms of AT13387, NVP-AUY922, and STA-9090 are shown in red and blue, respectively.

To rationally design a potent Hsp90 inhibitors, we first investigated crystal structures of Hsp90. To do so, we aligned three Hsp90 proteins (PDB codes: 2XJX, orange; 2VCI, cyan; 2TUH, yellow) and analyzed the ATP-binding site of the Hsp90 proteins with their Hsp90 inhibitors (AT13387, orange; NVP-AUY922, cyan; and STA-9090, yellow), all of which had been studied in clinical trials. Comparative structural analysis of the three Hsp90 proteins indicated that the ATP-binding site in the *N*-terminal domain consists of a hydrophilic region, a hydrophobic region, and an entry region (Figure 2A). The hydrophilic region is composed of Asn51, Asp93, and three conserved water molecules and the hydrophobic region consists of lipophilic amino acid residues, Leu107, Phe138, Trp162 and Val186. The hydrophilic and hydrophobic regions form a deep ATP-binding pocket in the *N*-terminal domain of Hsp90. In particular, the structure of the hydrophilic region is characterized by highly ordered amino acid residues and conserved water molecules in the pocket. The three conserved water molecules, along with the carboxylic acid terminus of Asp93 residue, form a hydrogen bonding network with the resorcinol ring of Hsp90 inhibitors. The deep cavity formed by the hydrophilic and hydrophobic regions plays a crucial role in the binding of the Hsp90 inhibitors. Enormous effort had therefore been directed toward the targeting of this deep cavity, and it was found that 4-isopropyl resorcinol scaffold tightly fits into the hydrophilic

and hydrophobic regions as a key binder. Unlike the hydrophilic and hydrophobic regions, the entry region is relatively flexible, and diverse scaffolds such as 4,5-diarylisoxazole, 1,3-dihydroisoindole, 4-indolyl-triazolone, and 5-aryl-1,2,3-triazole, have been studied to target the entry region. A structural analysis of AT13387 (orange), NVP-AUY922 (cyan), and STA-9090 (yellow) revealed that the binding poses of 4-isopropyl resorcinol ring in the ATP-binding pocket are highly ordered in the hydrophilic and hydrophobic regions, while the binding poses of the entry region binders are relatively disparate (Figure 2B).

To develop the Hsp90 inhibitors with a novel scaffold, an exploration of the diverse modifications of the entry region binder, while 4-chloro or 4-isopropylresorcinol ring was maintained as a key binder in the hydrophilic and hydrophobic regions, was conducted.

2.2. Chemistry

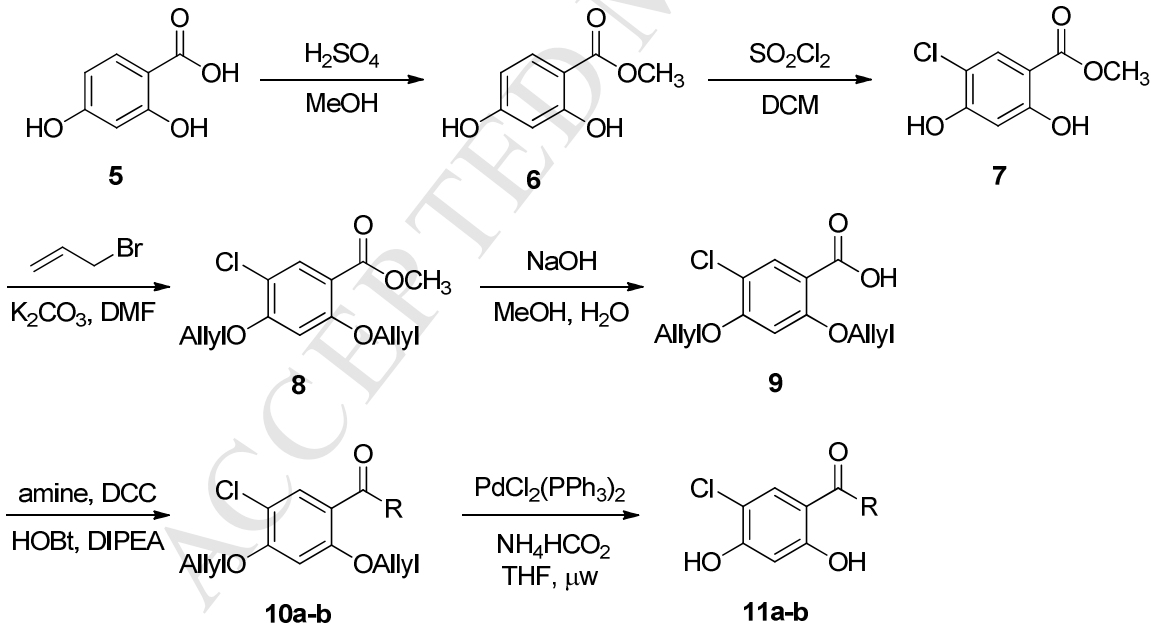

Scheme 1. Synthesis of compound **11a-b**.

We first decided to synthesize compounds **11a-b**, which had chloro group at C-5 of phenyl ring (Scheme 1). To do so, we pursued the synthesis of carboxylic acid **9** that was a key

intermediate in the synthetic plan. Methyl 2,4-dihydroxybenzoate (**6**) was synthesized from commercially available 2,4-dihydroxybenzoic acid (**5**) with a slight modification of the reported procedure [24]. Briefly, **5** was esterified in the presence of sulfuric acid in methanol to provide methyl 2,4-dihydroxybenzoate (**6**) in 86 % yield. Subsequent chlorination of **6** with sulfuryl chloride in dichloromethane furnished methyl 5-chloro-2,4-dihydroxybenzoate (**7**) in 45% yield, which was then protected with allyl bromide in the presence of potassium carbonate to give compound **8** in 100 % yield. Compound **8** was hydrolyzed to furnish carboxylic acid **9** in 80 % yield. With carboxylic acid **9** in hand, we next performed amide coupling reaction of carboxylic acid **9** with 1,2,3,4-tetrahydroisoquinoline and 4,5,6,7-tetrahydrothieno[3,2-c] pyridine and the reaction provided compound **10a-b** in 63 and 58 % yield, respectively. Finally, the removal of allyl-protecting groups, using $PdCl_2(PPh_3)_2$ and ammonium formate under microwave irradiation [25] furnished the resulting 5-chloro-2,4-hydroxybenzamides (**11a-b**) in 66 and 27 % yield. In this synthetic route, the yields of deprotection reactions were disappointingly low and the impurity of triphenylphosphine was also difficult to remove from the reaction mixture by flash column. Besides, the protection-deprotection event introduced two additional steps in the reaction sequence, and it needs to be minimized to achieve a green and atom-economic chemistry. Therefore, we investigated direct amide coupling reaction of 5-chloro-2,4-dihydroxybenzoic acid (**12**) without any protecting group (Scheme 2).

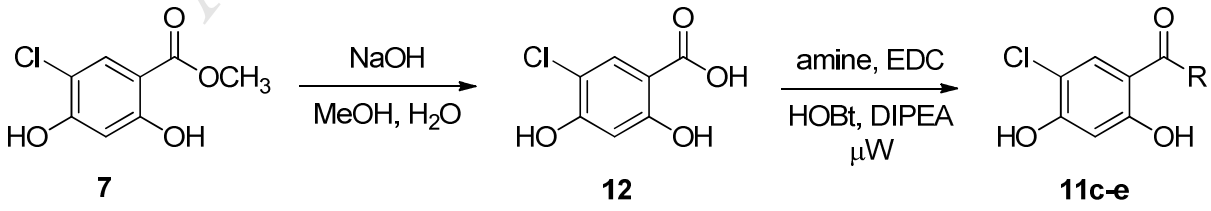

Scheme 2. Synthesis of compound **11c-e**.

To prepare carboxylic acid **12**, we carried out the hydrolysis reaction of ester **7** in the presence of sodium hydroxide in methanol and water to provide compound **12** in quantitative yield. With carboxylic acid **12** in hand, amide coupling reactions of carboxylic acid **12** with various amines were carried out using EDC under microwave irradiation to provide compound **11c-e** in 14-34% yield. Although the amide coupling reactions still provided unsatisfactory % yields, the synthetic route without the protection-deprotection steps resulted in an improvement of the overall yields.

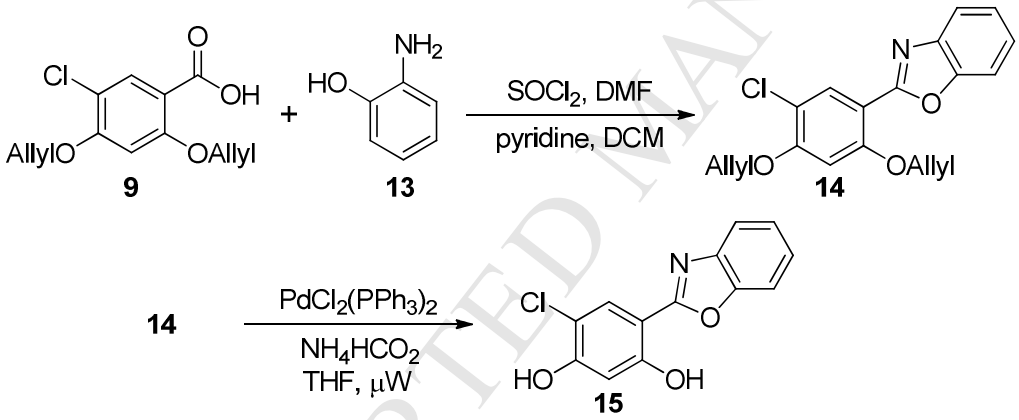

Scheme 3. Synthesis of compound **15**.

We next synthesized benzoxazole-containing compound **15**. Benzoxazole is an important class of heterocyclic compounds found in a number of anticancer agents. The synthesis of compound **15** is described in Scheme 3. The reaction of **9** with 2-aminophenol (**13**) was carried out in the presence of thionyl chloride, dimethyl formaldehyde, and pyridine to furnish **14** in 59% yield. The subsequent removal of the allyl-protecting groups, using $PdCl_2(PPh_3)_2$ and ammonium formate under microwave irradiation furnished compound **15** in 20% yield.

*2.3. In vitro assays of compounds **11a-e** and **15***

Table 1. Inhibitory activity against Hsp90α and cell growth inhibition against cancer cell lines

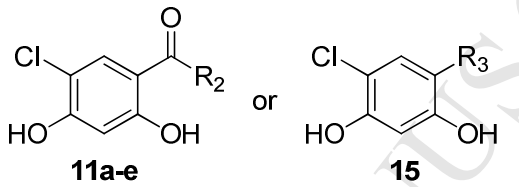

11a-e **15**

Compound	R_2	Hsp90α (FP)[a] (IC_{50}; nM)	H1975[b] (GI_{50}; μM)	Skbr3[c] (GI_{50}; μM)
11a	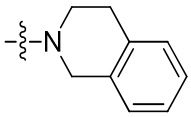	183.3	19.9	7.1
11b	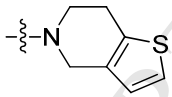	135.9	8.7	5.4
11c	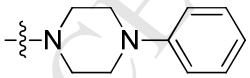	480.8	19.1	9.3
11d	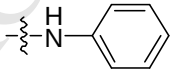	>1000	> 50	NA
11e	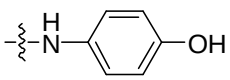	>1000	> 50	NA
15	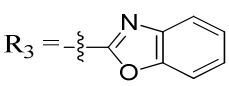	>1000	> 50	> 50

[a] Binding to *N*-terminal domain of Hsp90α was determined by a fluorescence polarization (FP) assay (14 h). [b] Cytotoxicity on H1975 non-small cell lung cancer cell (NSCLC) line. [c] Cytotoxicity on Skbr3 breast cancer cell line.

We next investigated the binding affinity of the resulting compounds (**11a-e** and **15**) to human recombinant Hsp90α and their anti-proliferative activity on two human cancer cell lines, H1975 and Skbr3, which are a gefitinib-resistant non-small cell lung cancer cell line and a Her2-overexpressing breast cancer cell line, respectively. As shown in Table 1, compounds **11a-c,** which had secondary amide groups, exhibited an appreciable binding affinity to human Hsp90α in a fluorescence polarization (FP) assay as well as good cellular efficacy against H1975 and Skbr3. Notably, analogue **11b** afforded the highest binding affinity (IC_{50} = 135.9 nM) to human Hsp90α in the FP assay compared with other analogues. Consistent with the result of Hsp90 binding assay, analogue **11b** also displayed the most potent anti-proliferative activity against the two cancer cell lines, H1975 and Skbr3. Interestingly, analogues **11d-e**, which had secondary amide groups, were unable to bind to human Hsp90α, so they did not show any cytotoxic effect on H1975 and Skbr3. Additionally, benzoxazole analogue **15** did not exhibit any activity in the FP assay or the cell growth inhibition assay. The resulting data indicated that the scaffold of the entry region binder was critical for the improvement of the binding affinity to the ATP-binding pocket of Hsp90. Nonetheless, compound **11b** afforded the highest binding affinity to human Hsp90α, and the most potent cellular efficacy in the two cancer cell lines, H1975 and Skbr3.

*2.4. Synthesis of compound **19***

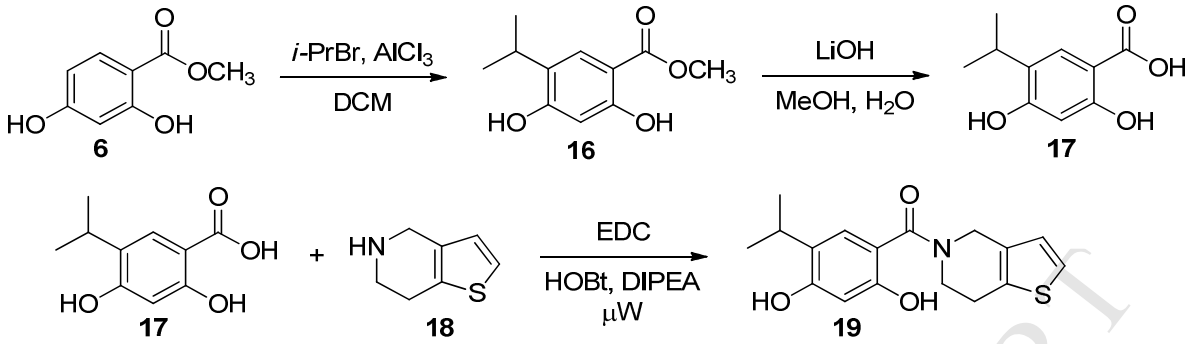

Scheme 4. Synthesis of compound **19**.

Encouraged by the potency conferred by compound **11b**, the synthesis of compound **19**, which contains an isopropyl group at C-5 of the phenyl ring, was embarked upon next. Isopropyl moiety is a common hydrophobic binder that is employed in the clinical development of resorcinol-based Hsp90 inhibitors. It has been reported that the replacement of the 5-chloro substituent with an isopropyl group in the resorcinol ring will increase the number of additional hydrophobic interactions in the hydrophobic region [21]. Accordingly, we pursued the synthesis of compound **19**. The synthetic route of compound **19** is illustrated in Scheme 4. The Friedel-Crafts alkylation of **6** with isopropyl bromide was carried out in the presence of aluminum chloride to provide methyl 1,4-dihydroxy-5-isopropylbenzoate (**16**) in 46% yield. A subsequent hydrolysis of **16** with lithium hydroxide in methanol and water provided carboxylic acid **17** in 100% yield. Lastly, the amide coupling reaction of **17** with commercially available secondary amine **18** using EDC afforded compound **19** in 52% yield.

*2.5. Comparative in vitro assays of compound **19** with geldanamycin and **11b***

Table 2. Inhibitory activity against Hsp90α and cell growth inhibition against cancer cell lines

Compound	Hsp90α (FP)[a] (IC_{50}; nM)	H1975[b] (GI_{50}; μM)	Skbr3[c] (GI_{50}; μM)	MW	cLogP

GA (**1**)	14.0	0.56	0.43	560	2.06
11b	135.9	8.7	5.4	309	2.61
19	50.3	0.31	0.11	317	3.32

[a] Binding to *N*-terminal domain of Hsp90α was determined by a fluorescence polarization (FP) assay (14 h). [b] Cytotoxicity on H1975 non-small cell lung cancer cell(NSCLC) line. [c] Cytotoxicity on Skbr3 breast cancer cell line.

With compound **19** in hand, we investigated the binding affinity of compound **19** to human Hsp90α and its cell growth inhibition activity on H1975 and Skbr3. As shown in Table 2, compound **19** afforded a significantly improved binding affinity to recombinant human Hsp90α protein in the FP assay with an IC_{50} value of 50.3 nM. It is noteworthy that the binding affinity of **19** is 2.7-fold higher than that of compound **11b** that has a chloro group at C-5 of the phenyl ring as a hydrophobic binder. As expected, isopropyl moiety retained a stronger binding affinity in the hydrophobic region than chloro moiety. The cell growth inhibitory effect of **19** was measured with H1975 and Skbr3 cancer cell lines using MTS colorimetric assay and it provided submicromolar GI_{50} values of 0.11 μM and 0.3 μM against H1975 and Skbr3 cell lines, respectively. Interestingly, according to the cell growth inhibition assay, the cellular efficacy of compound **19** (H1975 GI_{50} = 0.31 μM, Skbr3 GI_{50} = 0.11 μM) was 30 to 50 fold more active than **11b** (H1975 GI_{50} = 8.7 μM, Skbr3 GI_{50} = 5.4 μM) against H1975 and Skbr3 cancer cell lines. Considering that the binding affinity of **19** (IC_{50} = 50.3 nM) to Hsp90α protein in the FP assay was only 2.7 fold higher than that of **11b** (IC_{50} = 135.9 nM), it was assumed that compound **19** is more capable of penetrating into the cells than **11b,** affording highly active cellular efficacy against cancer cell lines. Furthermore, the difference of the hydrophobicity values between compound **19** (clogP = 3.32) and **11b** (clogP = 2.61) also supported this assumption. Importantly, compound **19** is more potent against

H1975 and Skbr3 than the reference compound GA in the cell growth inhibition assay. The ligand efficacy (LE), which refers to the potency per unit of the molecular weight, is considered to be an important criteria for judging the potential of the improvement in drug discovery. Through a comparison of the molecular weight of **19** (MW = 317) with that of GA (MW = 560), compound **19** has a high improvement potential in preclinical and clinical studies. Collectively, the advantage of isopropyl moiety over chloro moiety became apparent when the protein binding affinity, cellular growth inhibitory effect, and cell permeability were all considered.

*2.6. Molecular modeling of **19***

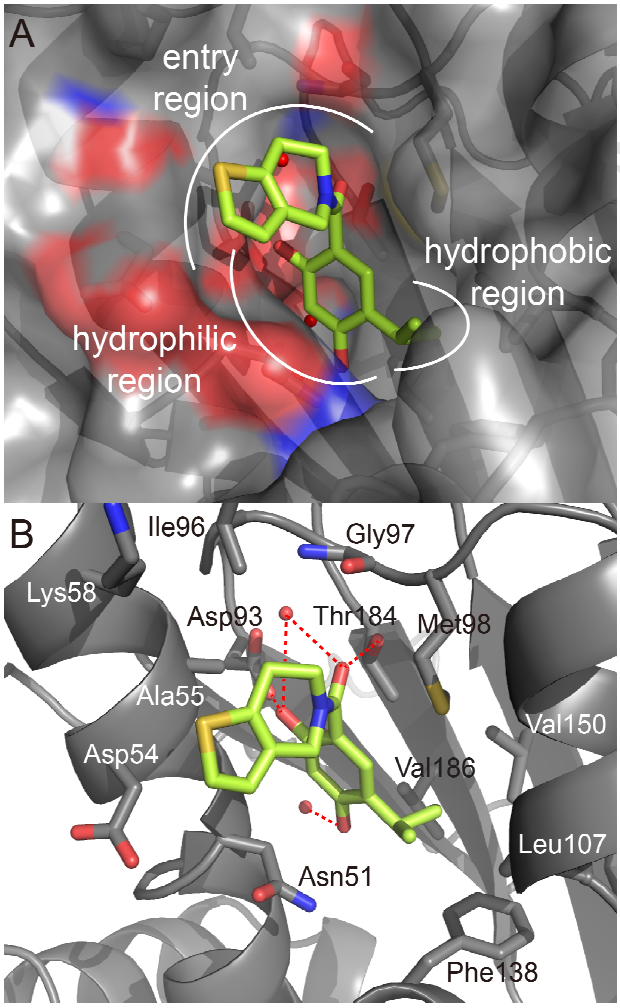

Figure 3. Molecular docking model of **19** bound in the ATP-binding pocket of human Hsp90

(PDB code: 2XJX). The carbon, oxygen, nitrogen, and sulfur atoms of **19** are shown in lime, red, blue, and yellow, respectively. The side chains of the binding site are colored according to the atom types (carbon, gray; oxygen, red; nitrogen, red) and are labeled with their residue name. The water molecules are shown as red spheres, and the hydrogen bonds are shown as dashed red lines. The docking poses were visualized using PyMOL1.3.

To assess the precise binding pose of compound **19** in the ATP-binding pocket of Hsp90α, we performed docking simulations of compound **19** using the *N*-terminal domain of Hsp90α (PDB code: 2XJX) as a template. The crystal structure of the ATP-binding pocket in the *N*-terminal domain of Hsp90α is characterized by a network of highly ordered water molecules in the hydrophilic region of the ATP-binding pocket. The docking study indicated that the resorcinol ring of **19** was located in the hydrophilic region as expected (Figure 3A). The carbonyl group of **19** formed two hydrogen bonding interactions with the hydroxyl group of Thr184 and a conserved water (Figure 3B). The hydroxyl group at C-2 of the phenyl ring also formed bidentate hydrogen bonding interactions with the carboxylate side chain of Asp93 as well as a conserved water and the hydroxyl group at C-4 interacted with one of the remaining conserved water molecule through hydrogen bonding. As the isopropyl group at C-5 of **19** had been designed as a hydrophobic binder, the isopropyl group could project into the hydrophobic region, and it efficiently formed proximal Van der Waals interactions with lipophilic residues of Val186, Val150, Leu107, and Phe138. The 6,7-Dihydrothieno[3,2-c]pyridin-5(4H)-yl moiety of compound **19**, which was selected as the most potent entry region binder among analogues in Tables 1 and 2, is nicely positioned in the entry region of the ATP-binding pocket (Figure 3A). This entry region binder formed proximal Van der Waals contacts with the hydrophobic side chains of Ala55 and Ile96 as well as the β-carbon of Asp54.

*2.6. Biological evaluation of **19***

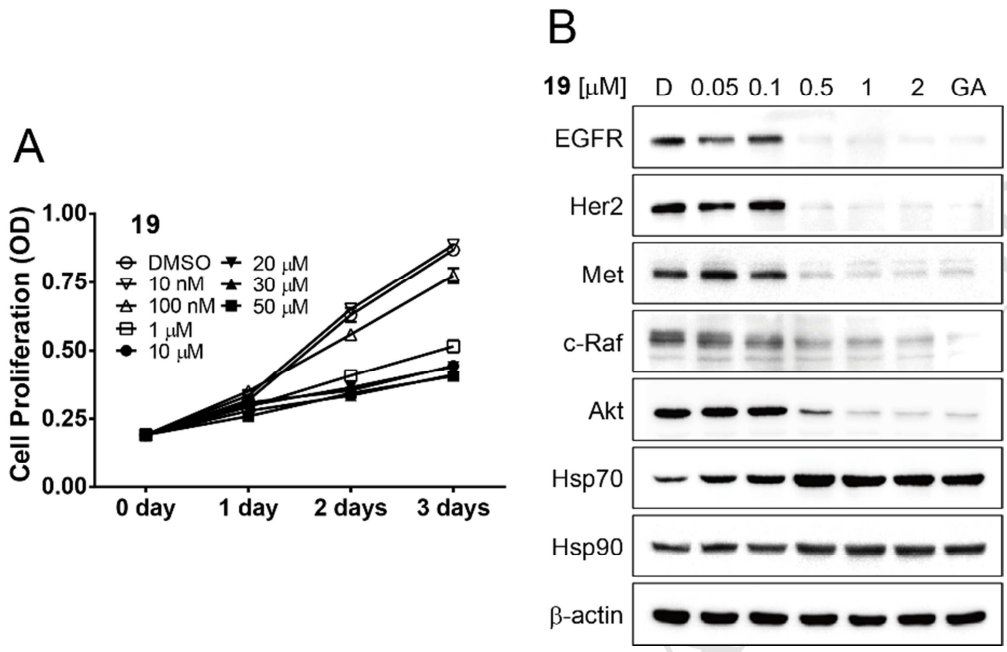

Figure 4. (A) Effect of compound **19** on the cell proliferation of H1975. Cells were incubated with the indicated concentration of **19** for 0, 1, 2, and 3 days and cell proliferation was measured using the MTS assay. Data are presented as mean ± SD (n = 4). (B) Effect of compound **19** on the expression of EGFR, Her2, Met, c-Raf, Akt, Hsp70 and Hsp90. H1975 cells were incubated with the indicated concentrations of **19** for 24 h and the expression of the Hsp90 client proteins were analyzed using the western blot. Geldanamycin (GA, 1 μM) and DMSO (D) were employed as a positive and a negative control, respectively.

To investigate the dose- and time-dependent anti-proliferative effect of compound **19**, H1975 cells were treated with compound **19** at various concentrations (0, 0.01, 0.1, 1, 10, 20, 30, 50 μM) for 0, 1, 2, and 3 days. Expectedly, the data indicated that compound **19** afforded a potent growth-inhibitory effect of H1975 cells in a dose- and time-dependent manner (Figure 4A). Compound **19** almost completely impaired the growth of H1975 cells at the concentration

of 1 μM.

To add support to the premise that compound **19** exerts its anti-proliferative effect via Hsp90 inhibition, we next studied the cellular biomarkers of Hsp90 inhibition. Hsp90 is responsible for maintaining the stability of EGFR, Her2, Met, c-Raf, and Akt. Hence, an inhibition of the Hsp90 function will promote the degradation of these client proteins via the ubiquitin-proteasome pathway. As shown in Figure 4B, the exposure of H1975 cells to **19** caused a significant reduction in the cellular protein levels of EGFR, Her2, Met, c-Raf, and Akt, while compound **19** upregulated the cellular protein level of Hsp70, which is considered a cellular hallmark of Hsp90 inhibition. The expression level of non-Hsp90-dependent protein, β-actin remained unchanged. Collectively, the results indicated that compound **19** disrupted the Hsp90 chaperone function and circumvented the gefitinib-resistance in H1975 cells through a destabilizing of oncogenic proteins such as EGFR, Her2, Met, c-Raf, and Akt.

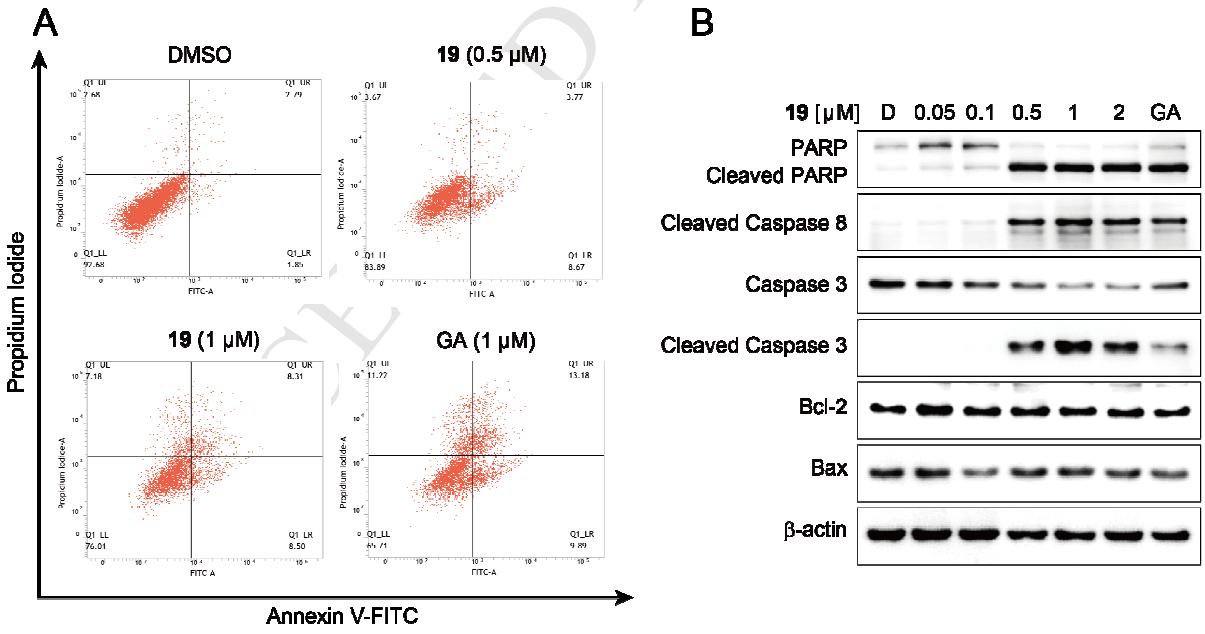

Figure 5. Compound **19** induces apoptosis in H1975 cells. (A) H1975 cells were treated with compound **19** (0.5 and 1 μM) for 24 h, and they were then analyzed using flow cytometric analysis with Annexin V and propidium iodide staining. (B) H1975 cells were incubated with

compound **19** (0, 0.05, 0.1, 0.5, 1, and 2 μM) for 24 h and the expression of the apoptotic biomarker proteins (PARP, cleaved caspase 8, caspase 3, cleaved caspase 3, Bcl-2, and Bax) was analyzed using the western blot. Geldanamycin (GA, 1 μM) and DMSO (D) were employed as a positive and a negative control, respectively.

The proliferation of cancer cells can be suppressed by the activation of apoptotic signals, as it is regulated by the avoidance of the apoptosis mechanism. To determine whether the anti-proliferative effect of compound **19** on H1975 cells is related to the induction of apoptosis, we treated H1975 cells with compound **19** (0.5 and 1 μM) for 24 h. The cells were then stained with Annexin V and propidium iodide, and they were analyzed using fluorescence-activated cell sorting (FACS). As shown in Figure 5A, the treatment of H1975 cells with **19** remarkably induced early and late apoptosis at the level of 8.5 and 8.3%, respectively. As an additional approach for the assessment of apoptosis, the effect of compound **19** on apoptotic-biomarker proteins such as PARP, caspase8, caspase3, B-cell lymphoma 2 (Bcl-2), and Bcl-2-associated X protein (Bax) was investigated, as shown in Figure 5B. The exposure of H1975 cell to 0.5 μM of **19** induced the cleavage of PARP, caspase 8, and caspase 3 that indicated that compound **19** promoted apoptotic cell death even at the concentration of 0.5 μM. Interestingly, compound **19** did not alter the expression levels of Bcl-2 and Bax. It is probably because compound **19** activates the apoptosis of H1975 cells through the extrinsic apoptotic pathway. Nonetheless, the results clearly suggest that compound **19** efficiently inhibits the growth of H1975 cells through inducing apoptosis.

*2.7. Effect of **19** on cytochrome P450s*

Table 3. Inhibitory potency of compound **19** on specific P450 activities in human liver microsomes

Enzyme activity	P450	IC_{50} (μM)
Phenacetin *O*-deethylation	1A2	> 50
Tolbutamide 4-methylhydroxylation	2C9	> 50
Omepraozle hydroxylation	2C19	> 50
Dextromethorphan *O*-demethylation	2D6	> 50
Midazolam 1'-hydroxylation	3A	> 50

Cytochrome P450 (P450) enzymes are essential for the metabolism of many drugs and drug metabolism via the cytochrome P450 system has emerged as an important determinant in the occurrence of drug interactions that can lead to drug toxicities, reduced pharmacological effect, and adverse drug reactions. Therefore, we investigated the effect of compound **19** on the catalytic activities of clinically significant human P450s such as 1A2, 2C9, 2C19, 2D6, and 3A in human liver microsomes [26]. To do so, the inhibitory potency of compound **19** was determined with cytochrome P450 assays in the absence and presence of compound **19** up to 50 μM final concentration using pooled human liver microsomes. The assay indicated that compound **19** had no effect on the activities of five major P450 isoforms and all of the IC_{50} values for these enzymes were higher than 50 μM. These findings suggest that clinical interactions between compound **19** and the substrate drugs of these P450 isoforms are not expected.

*2.8. In vivo anticancer effect of **19***

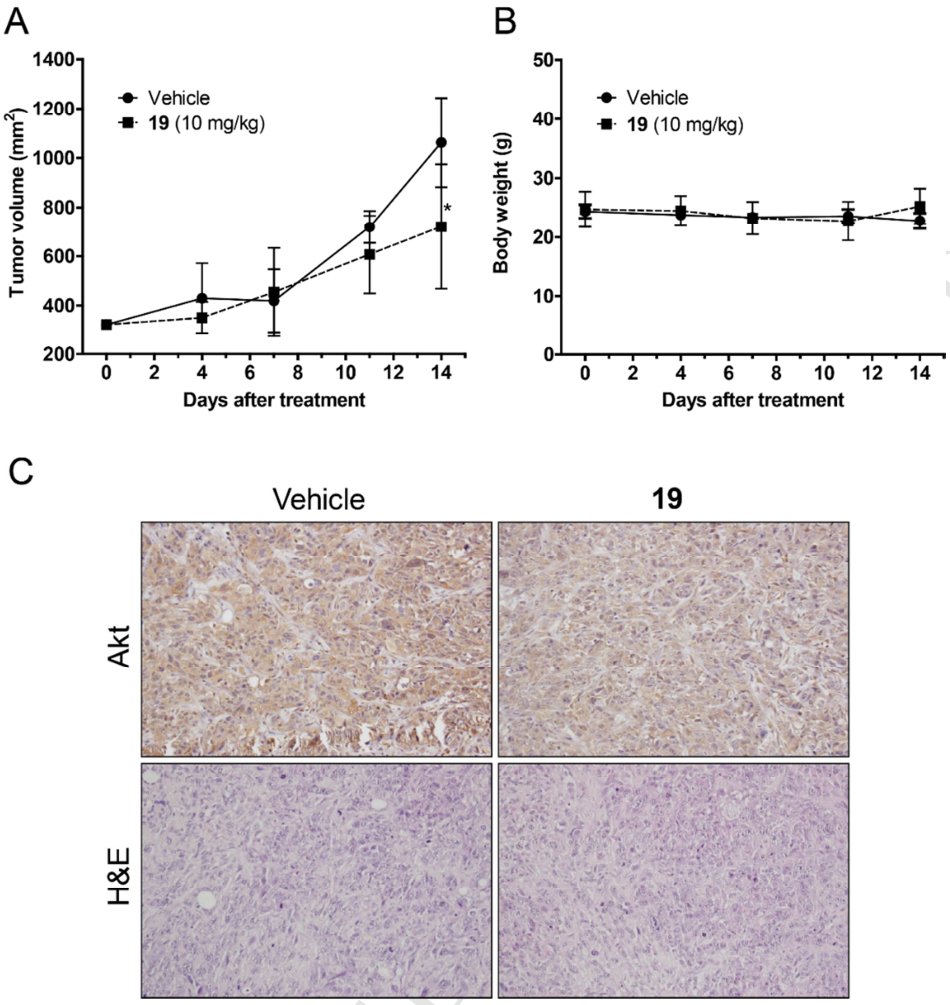

Figure 6. Antitumor activity of compound **19** in a mouse xenograft model. (A) The average volumes of the H1975-derived tumors from the vehicle and compound **19** treated mice were plotted 10 days after tumor inoculations. Statistical significance was determined by the Student's t-test (*p<0.05, **p<0.01, ***p<0.001). (B) Body weight changes were recorded during the treatment of vehicle and compound **19**. (C) Immunostaining of H&E and akt in H1975 xenograft tissue sections.

To confirm that *in vitro* anticancer effect of **19** translates into *in vivo* model, we subcutaneously injected NOD-scid IL2Rgamma^{null} mice (NSG) mice with H1975 human non-small lung cancer cells and compound **19** or vehicle control was intraperitoneally

administered to mice bearing subcutaneous tumors daily followed by weekend rest for 2 weeks at 10 mg/kg. Mice injected with vehicle control rapidly developed visible tumors that grew continuously throughout the course of the treatment period. In contrast, mice injected with compound **19** exhibited a delayed growth of the tumors that are significantly smaller in size compared with those of vehicle control (Figure 6A). On the basis of body weight measurements, compound **19** was well tolerated at the dose level of 10 mg/kg during the course of the treatment period and no treatment-related deaths were observed. The morphology of xenotransplanted tumor defined epitheloid tumor features similar to those of human epithelial lung cancer. In agreement of *in vitro* results, we also observed decreased Akt expression in tumor samples treated with compound **19** (Figure 6C).

3. Conclusions

In summary, the discovery and characterization of the novel Hsp90 inhibitor **19** has been described. Systematic analysis of multiple X-ray co-crystal structures enabled the design and optimization of the novel class of Hsp90 inhibitor **19**. The overall synthetic schemes developed in this study allowed for an easy preparation of the intermediates and the diverse analogues. In addition, its practical synthetic route made it readily amenable to large scale synthesis. Compound **19** demonstrated an exceptionally potent binding affinity to the *N*-terminus of Hsp90α in the FP assay (IC_{50} = 50.3 nM). The docking simulation demonstrated that compound **19** tightly occupied the ATP-binding pocket in the *N*-terminal domain of Hsp90α, hereby supporting the strong binding affinity of **19** to Hsp90α that was observed in the FP assay. The strong enzyme affinity of compound **19** agreeably translated into good cellular activity, whereby compound **19** inhibited the proliferation of H1975 NSCLC and Skbr3 breast cancer cell lines with GI_{50} values of 0.31 μM and 0.11 μM, respectively. The exposure of cancer cells to compound **19** displayed the characteristic molecular biomarkers of

Hsp90 inhibition such as the downregulation of oncogenic proteins (EGFR, Her2, Met, c-Raf, and Akt) and the upregulation of Hsp70. The results of FACS and western blot analysis indicated that compound **19** inhibited the growth of H1975 cells through the inducement of apoptosis. Cytochrome P450 assay indicated that compound **19** had no effect on the activities of five major P450 isoforms (IC_{50} > 50 μM for 1A2, 2C9, 2C19, 2D6, and 3A), suggesting that clinical interactions between compound **19** and these P450 isoforms are not expected. Moreover, compound **19** displayed a significant *in vivo* efficacy in a mouse xenograft model bearing subcutaneous H1975 tumors and the immunostaining of H&E and Akt in xenograft tissue sections is in a good agreement with the *in vitro* results. Overall, the attractive attributes of **19** warranted further studies on ADMET profile and its therapeutic evaluation for various types of cancer. These studies will be reported in due course.

4. Experimental

4.1. Chemistry

4.1.1. Methyl 2,4-dihydroxybenzoate (6)

2,4-Dihydroxybenzoic acid (10 g, 64.88 mmol) and sulfuric acid (5 mL) in MeOH (40 mL) was stirred at 100℃ for 24 h, equipped with a refluxing condenser under argon. After cooling at room temperature, the mixture was concentrated under reduced pressure and added water at 0 ^{o}C. To filter the resulting white solid was dissolved in ethyl acetate washed with saturated $NaHCO_3$ solution. The organic layer was dried over Na_2SO_4, concentrated under reduced pressure to afford compound **6** in 86% yield. ^{1}H NMR (500 MHz, CD_3OD) 7.56 (d, *J* = 9 Hz, 1H), 6.24 (dd, *J* = 8.8 Hz, 2.0 Hz, 1H), 6.21 (d, *J* = 2.5 Hz, 1H), 3.78 (s, 3H). ^{13}C NMR (125 MHz, CD_3OD) δ 171.7, 165.7, 164.9, 132.7, 109.1, 105.5, 103.4, 52.3.

4.1.2. Methyl 5-chloro-2,4-dihydroxybenzoate (7)

A mixture of compound **6** (10.0 g, 59.5 mmol) and sulfuryl chloride (4.30 mL, 59.5 mmol) in CH_2Cl_2 was stirred at 0 ^oC for 24 h under argon. The mixture was neutralized with 10 % NaOH to pH 5, concentrated under reduced pressure, and then extracted with ethyl acetate. The organic layer was washed with saturated $NaHCO_3$ solution three times, dried over Na_2SO_4, concentrated under reduced pressure, and purified by column to afford compound **7** in 45% yield. R_f = 0.26 (2:8 ethyl acetate: hexane). ^1H NMR(400 MHz, $CDCl_3$) δ 10.83 (s, 1H), 7.82 (s, 1H), 6.61 (s, 1H), 5.94 (s, 1H), 3.92 (s, 3H). ^{13}C NMR (100 MHz, $CDCl_3$) δ 169.6, 162.5, 157.3, 130.3, 111.5, 106.8, 104.3, 52.6.

4.1.3. Methyl 2,4-bis(allyloxy)-5-chlorobenzoate (8)

A mixture of compound **7** (6.09 g, 30.00 mmol), allyl bromide (6.75 ml, 78.02 mmol) and potassium carbonate (10.78 mL, 78.02 mmol) in DMF was stirred at room temperature for 24 h under argon. The mixture was concentrated under reduced pressure, and then extracted with ethyl acetate. The organic layer was washed with saturated $NaHCO_3$ solution three times, dried over Na_2SO_4 and concentrated under reduced pressure to afford compound **8** in 100% yield. ^1H NMR (400 MHz, $CDCl_3$) δ 7.85 (s, 1H), 7.25 (s, 1H), 6.44 (s, 1H), 6.44-5.95 (m, 2H), 5.52-5.40 (m, 2H), 5.31-5.29 (m, 2H), 4.58-4.54 (m, 4H), 3.82 (s, 3H). ^{13}C NMR (100 MHz, $CDCl_3$) δ 164.7, 158.7, 157.7, 133.0, 132.2, 131.7, 118.1, 117.4, 113.9, 112.6, 99.4, 69.7, 51.7.

4.1.4. 2,4-Bis(allyloxy)-5-chlorobenzoic acid (9)

A mixture of compound **8** (9.43 g, 37.99 mmol) and sodium hydroxide (5 g) in methanol (25 mL) - H_2O (25 mL) was stirred at room temperature for 30 h. The mixture was neutralized with 1N HCl to pH 6 and then extracted with ethyl aceatate three times. The organic layer was dried over Na_2SO_4, concentrated under reduced pressure to afford compound **9** in 80%

yield. ^{1}H NMR (400 MHz, $CDCl_3$) δ 8.16 (s, 1H), 6.55 (s, 1H), 6.10-5.99 (m, 2H), 5.51-5.35 (m, 2H), 4.77-4.66 (m, 4H). ^{13}C NMR (125 MHz, $CDCl_3$) δ 164.5, 158.9, 157.3, 134.7, 131.7, 130.8, 120.9, 118.9, 116.9, 111.3, 98.9, 71.4, 70.2..

4.1.5. (5-Chloro-2,4-dihydroxyphenyl)(3,4-dihydroisoquinolin-2(1H)-yl)methanone (11a)

A mixture of compound **9** (0.3 g, 1.12 mmol), 1,2,3,4-tetrahydroisoquinoline (0.21 mL, 1.68 mmol), *N,N'*-dicyclohexylcarboiimide (0.46 g, 2.23 mmol), hydroxybenzotriazole (0.15 g, 1.12 mmol), *N,N*-diisopropylethylamine (0.20 mL, 1.12 mmol) in 3 mL of DMF was stirred under microwave irradiation for 3h at 80 ^{o}C. The mixture was dissolved in ethyl acetate. The organic layer was washed with water, dried over Na_2SO_4, concentrated under reduced pressure and purified by MPLC to afford intermediate compound. R_f = 0.30 (3:7 ethyl acetate: hexane). The resulting intermediate compound was stirred under microwave irradiation for 1 h at 120 ^{o}C in the presence of Pd $Cl_2(PPh_3)_2$ (37 mg) and ammonium formate (300 mg) in 3 mL of THF. The reaction mixture was diluted with ethyl acetate. The organic layer was washed with water, dried over Na_2SO_4,concentrated under reduced pressure and purified by MPLC to afford compound **11a** in 66% yield in two steps. R_f = 0.20 (2:3 ethyl acetate: hexane). ^{1}H NMR (500 MHz, $CDCl_3$) δ 7.35 (s, 1H), 7.23-7.18 (m, 3H), 7.13-7.12 (m, 1H), 6.67 (s, 1H), 4.82 (s, 2H), 3.90 (t, *J* = 6.0 Hz, 2H), 3.00 (t, *J* = 6.0 Hz, 2H). ^{13}C NMR (125 MHz, $CDCl_3$) δ 170.7, 160.9, 155.0, 134.3, 132.5, 128.9, 128.5, 127.2, 126.8, 126.5, 110.7, 110.1, 105.3, 48.6, 44.4, 28.9. ESI MS (*m/e*) 304.07 $[M+1]^{+}$.

4.1.6. (5-Chloro-2,4-dihydroxyphenyl)(4,5-dihydrothieno[2,3-c]pyridin-6(7H)-yl)methanone (11b)

A mixture of compound **9** (0.3 g, 1.12 mmol), 4,5,6,7-terahydrothieno[3,2-c] pyridine hydrochloride (0.29 g, 1.68 mmol), *N,N'*-dicyclohexylcarboiimide (0.46 g, 2.23 mmol),

hydroxybenzotriazole (0.15 g, 1.12 mmol), *N*,*N*-diisopropylethylamine (0.20 mL, 1.12 mmol) in 3 mL of DMF was stirred under microwave irradiation for 3h at 80 ^{o}C. The mixture was dissolved in ethyl acetate. The organic layer was washed with water, dried over Na_2SO_4, concentrated under reduced pressure and purified by MPLC to afford intermediate compound. R_f = 0.23 (1:3 ethyl acetate: hexane). The resulting intermediate compound was stirred under microwave irradiation for 1 h at 120 ^{o}C in the presence of Pd $Cl_2(PPh_3)_2$ (50 mg) and ammonium formate (500 mg) in 3 mL of THF. The reaction mixture was diluted with ethyl acetate. The organic layer was washed with water, dried over Na_2SO_4,concentrated under reduced pressure and purified by MPLC to afford compound **11b** in 27% yield in two steps. R_f = 0.26 (2:3 ethyl acetate: hexane). ^{1}H NMR (400 MHz, $CDCl_3$) δ 10.26 (s, 1H), 7.32 (s, 1H), 7.16 (d, *J* = 5.2 Hz, 1H), 6.78 (d, *J* = 5.2 Hz, 1H), 6.65 (s, 1H), 6.13 (s, 1H), 4.76 (s, 2H), 3.95 (t, *J* = 6.0 Hz, 2H), 3.03 (t, *J* = 5.6 Hz, 2H). ^{13}C NMR (125 MHz, $CDCl_3$) δ 171.1, 161.0, 155.1, 133.4, 131.5, 128.4, 124.8, 124.1, 110.7, 110.2, 105.4, 47.5, 44.2, 25.1. ESI MS (*m/e*) 310.88 $[M+1]^{+}$.

4.1.7. (5-Chloro-2,4-dihydroxyphenyl)(4-phenylpiperazin-1-yl)methanone (11c)

A mixture of compound **12** (0.17 g, 0.90 mmol), 1-phenylpiperazine (0.21 mL, 1.50 mmol), 1-ethyl-3-(3-dimethylaminopropyl)carbodiimide (0.35 g, 1.80 mmol), hydroxybenzotriazole (0.12 g, 0.90 mmol), *N*,*N*-diisopropylethylamine (0.16 mL, 0.90 mmol) in 3 mL of DMF was stirred under microwave irradiation for 3h at 120 ^{o}C. The mixture was dissolved in ethyl acetate. The organic layer was washed with 1N-HCl solution, dried over Na_2SO_4, concentrated under reduced pressure and purified by MPLC to afford compound **11c** in 14% yield in two steps. R_f = 0.23 (2:3 ethyl acetate: hexane). ^{1}H NMR (500 MHz, $CDCl_3$) δ 10.13(s, 1H), 7.30-7.26(m, 2H), 6.94-6.93(br, 3H), 6.66(s, 1H), 5.77(s, 1H), 3.88(s, 4H), 3.24(t, *J* = 5.0 Hz, 4H). ^{13}C NMR (150 MHz, $CDCl_3$) δ 170.3, 160.9, 155.0, 150.7, 129.4,

128.6, 120.9, 116.7, 110.2, 110.1, 105.3, 59.5, 49.7, 46.0, 31.0. ESI MS (*m/e*) 333.10 $[M+1]^+$.

4.1.8. 5-Chloro-2,4-dihydroxy-N-phenylbenzamide (11d)

A mixture of compound **12** (0.30 g, 1.59 mmol), aniline (0.22 mL, 2.39 mmol), 1-ethyl-3-(3-dimethylaminopropyl)carbodiimide (0.61 g, 3.18 mmol), hydroxybenzotriazole (0.21 g, 1.59 mmol), *N*,*N*-diisopropylethylamine (0.28 mL, 1.59 mmol) in 3 mL of DMF was stirred under microwave irradiation for 3h at 120 ^oC. The mixture was dissolved in ethyl acetate. The organic layer was washed with 1N-HCl solution, dried over Na_2SO_4, concentrated under reduced pressure and purified by column to afford compound **11d** in 37% yield in two steps. R_f = 0.23 (3:7 ethyl acetate: hexane). ^1H NMR (400 MHz, CD_3OD) δ 7.88 (s, 1H), 7.53 (d, *J* = 8.4 Hz, 2H), 7.22 (t, *J* = 7.6 Hz, 2H), 7.01 (t, *J* = 7.4 Hz, 1H), 6.36 (s, 1H). ^{13}C NMR (100 MHz, CD_3OD) δ 166.7, 159.9, 157.8, 137.7, 129.4, 128.4, 128.0, 124.2, 121.5, 121.1, 111.8, 109.0, 103.6. ESI MS (*m/e*) 286.82 $[M+Na]^+$.

4.1.9. 5-Chloro-2,4-dihydroxy-N-(4-hydroxyphenyl)benzamide (11e)

A mixture of compound **12** (0.30 g, 1.59 mmol), 4-aminophenol (0.26 g, 2.39 mmol), 1-ethyl-3-(3-dimethylaminopropyl)carbodiimide (0.61 g, 3.18 mmol), hydroxybenzotriazole (0.21 g, 1.59 mmol), *N*,*N*-diisopropylethylamine (0.28 mL, 1.59 mmol) in 3 mL of DMF was stirred under microwave irradiation for 3h at 120 ^oC. The mixture was dissolved in ethyl acetate. The organic layer was washed with 1N-HCl solution, dried over Na_2SO_4, concentrated under reduced pressure and purified by MPLC to afford compound **11e** in 34% yield in two steps. R_f = 0.16 (3:7 ethyl acetate: hexane). ^1H NMR (400 MHz, CD_3OD) δ 7.87 (s, 1H), 7.32 (d, *J* = 8.8 Hz, 2H), 6.71 (d, *J* = 8.8 Hz, 2H), 6.41 (s, 1H). ^{13}C NMR (100 MHz, CD_3OD) δ 168.2, 161.4, 159.0, 155.8, 130.7, 130.5, 124.9, 124.8, 116.3, 113.1, 110.3, 105.1. ESI MS (*m/e*) 280.04 $[M+1]^+$.

4.1.10. 5-chloro-2,4-dihydroxybenzoic acid (12)

A mixture of compound **9** (1.98 g, 9.76 mmol) and sodium hydroxide (6 g) in methanol (30 mL) - H_2O (30 mL) was stirred at room temperature for 24 h. The mixture was neutralized with 3N HCl to pH 6 and then extracted with ethyl aceatate three times. The organic layer was dried over Na_2SO_4, concentrated under reduced pressure to afford compound **12** in 100% yield. ^{1}H NMR (400 MHz, $CDCl_3$) δ 7.75 (s, 1H), 6.40 (s, 1H). ^{13}C NMR (100 MHz, CD_3OD) δ 171.5, 163.6, 160.6, 131.3, 113.0, 106.6, 104.4.

4.1.11. 4-(Benzo[d]oxazol-2-yl)-6-chlorobenzene-1,3-diol (15)

A mixture of thionyl chloride (0.2 mL, 2.69 mmol) and DMF (0.21 mL, 2.69 mmol) in DCM (30 ml) and added compound **9** (0.33 g, 1.22 mmol) in DCM (4mL) was stirred under argon for 20 min. After added 2-aminophenol (0.13g, 1.22mmol) in DCM, pyridine (0.59 mL, 7.32 mmol) was added dropwise and stirred for 12h. The mixture was dissolved in DCM. The organic layer was washed with 1N-HCl solution, dried over Na_2SO_4, concentrated under reduced pressure and purified by MPLC to afford intermediate compound. R_f = 0.33 (3:7 ethyl acetate: hexane). The resulting intermediate compound was stirred under microwave irradiation for 30 min at 120 ^{o}C in the presence of Pd $Cl_2(PPh_3)_2$ (20 mg) and ammonium formate (200 mg) in 3 mL of THF. The reaction mixture was diluted with ethyl acetate. The organic layer was washed with water, dried over Na_2SO_4,concentrated under reduced pressure and purified by MPLC to afford compound **15** in 20% yield in two steps. R_f = 0.23 (3:7 ethyl acetate: hexane). ^{1}H NMR (400 MHz, $CDCl_3$) δ 7.98 (s, 1H), 7.70-7.68 (m, 1H), 7.59-7.56 (m, 1H), 7.37-7.24 (m 2H), 6.76 (s, 1H). ^{13}C NMR (100 MHz, $CDCl_3$) δ 161.9, 159.4, 155.5, 148.9, 139.9, 127.0, 125.3, 125.1, 119.1, 111.7, 110.6, 105.0, 104.5. ESI MS (*m/e*) 284.19 $[M+Na]^+$.

4.1.12. Methyl 2,4-dihydroxy-5-isopropylbenzoate (16)

A mixture of compound **6** (3.9 g, 23.0 mmol), 2-bromopropane (4.3 mL, 46.0 mmol), and aluminum chloride (6.1 g, 46.0 mmol) in CH_2Cl_2 was stirred at 50 ^oC for 24 h , equipped with a refluxing condenser under argon. 2-Bromopropane (4.3 mL, 46.0 mmol) was added to the reaction mixture three times every 6 hours. The mixture was neutralized with 10% NaOH to pH 5, concentrated under reduced pressure, and then extracted with ethyl aceatate. The organic layer was washed with saturated $NaHCO_3$ solution three times, dried over Na_2SO_4, concentrated under reduced pressure, and purified by column to afford compound **16** in 45% yield. R_f = 0.21 (1:4 ethyl acetate: hexane). ^1H NMR (400 MHz, $CDCl_3$) δ 10.8 (s, 1H), 7.64 (s, 1H), 6.34 (s, 1H), 5.50 (s, 1H), 3.90 (s, 3H), 3.15-3.08 (m, 1H), 1.25 (d, *J* = 10.8 Hz, 6H). ^{13}C NMR (100 MHz, $CDCl_3$) δ 170.7, 161.6, 159.6, 128.1, 127.1, 105.7, 103.2, 52.2, 26.7, 22.8.

4.1.13. 2,4-Dihydroxy-5-isopropylbenzoic acid (17)

A mixture of compound **16** (0.24 g, 0.97 mmol) and lithium hydroxide (1 g) in methanol (10 mL) - H_2O (10 mL) was stirred at 50 ^oC for 12 h , equipped with a refluxing condenser under argon.. The mixture was neutralized with 6N HCl to pH 6 and then extracted with ethyl acetate three times. The organic layer was dried over Na_2SO_4, concentrated under reduced pressure and purified by MPLC to afford compound **17** in 100 % yield. R_f = 0.23 (3:7 ethyl acetate: hexane). ^1H NMR (400 MHz, CD_3OD) δ 7.68 (s, 1H), 6.35 (s, 1H), 3.25-3.22 (m, 1H), 1.27 (d, *J* = 4.0 Hz, 6H). ^{13}C NMR (100 MHz, CD_3OD) δ 173.8, 163.3, 163.1, 129.2, 128.7, 105.4, 103.1, 27.7, 23.2.

4.1.14. (6,7-Dihydrothieno[3,2-c]pyridin-5(4H)-yl)(2,4-dihydroxy-5-

isopropylphenyl)methanone (19)

A mixture of compound **17** (0.50 g, 2.55 mmol), 4,5,6,7-tetrahydrothieno[3,2-c]pyridine hydrochloride (0.67 ml, 3.82 mmol), 1-ethyl-3-(3-dimethylaminopropyl)carbodiimide (0.98 g, 5.09 mmol), hydroxybenzotriazole (0.34 g, 2.55 mmol), *N*,*N*-diisopropylethylamine (0.91 mL, 5.09 mmol) in 4 mL of DMF was stirred under microwave irradiation for 4h at 120 ^{o}C. The mixture was dissolved in ethyl acetate. The organic layer was washed with 1N-HCl solution, dried over Na_2SO_4, concentrated under reduced pressure and purified by MPLC to afford compound **19** in 52% yield. R_f = 0.27 (3:7 ethyl acetate: hexane). ^{1}H NMR (500 MHz, $(CD_3)_2CO$) δ 10.18(s, 1H), 8.90 (s, 1H), 7.27 (d, *J* = 5.0 Hz, 1H), 7.24 (s, 1H), 6.87 (d, *J* = 5.5 Hz, 1H), 6.24 (s, 1H), 4.74 (s, 2H), 3.94 (t, *J* = 5.5 Hz, 6.0 Hz, 2H), 3.25-3.01 (m, 1H), 3.02 (t, *J* = 6.0 Hz, 5.5 Hz, 2H), 1.22 (d, *J* = 7.0 Hz, 6H). ^{13}C NMR (125 MHz, $(CD_3)_2CO$) 172.8, 159.8, 159.3, 134.1, 133.3, 127.4, 126.8, 126.0, 124.4, 110.1, 103.9, 47.1, 45.2, 27.1, 25.8, 23.0. ESI MS (*m/e*) 318.12 $[M+1]^+$.

4.2. Molecular Modeling

In silico docking of **19** with the 3D coordinates of the X-ray crystal structures of the *N*-terminal domain of human Hsp90 ((PDB code: 2XJX) was accomplished using the AutoDock program downloaded from the Molecular Graphics Laboratory of the Scripps Research Institute. In the docking experiments carried out, gasteiger charges were placed on the X-ray structures of the *N*-terminal domain of Hsp90 along with **19** using tools from the AutoDock suite. A grid box centered on the *N*-terminal Hsp90 domain with definitions of 60_60_60 points and 0.375 Å spacing was chosen for ligand docking experiments. The docking parameters consisted of setting the population size to 150, the number of generations to 27000, and the number of evaluations to 25000000, while the number of docking runs was set to 50 with a cutoff of 1 Å for the root-mean-square tolerance for the grouping of each

docking run. The docking model of human Hsp90 with compound **19** was depicted in Figure 3 and rendering of the picture was generated using PyMol (DeLano Scientific).

4.3. Biology

4.3.1. Cell culture

Skbr3 and H1975 cells were grown in RPMI 1640 (containing 25 mM HEPES) and RPMI 1640 with L-glutamine supplemented with streptomycin (500 mg/mL), penicillin (100 units/mL), and 10% fetal bovine serum (FBS). Cells were grown to confluence in a humidified atmosphere (37 ^{o}C, 5% CO_2).

4.3.2. Cell proliferation assay

Cells were seeded at 3×10^3 (Skbr3), 2×10^3 (H1975) cells per well in a clear 96-well plate, the medium volume was brought to 100 μL, and the cells were allowed to attach overnight. The next day, varying concentrations of **11a-e, 15, 19** (Skbr3and H1975) or 1 % DMSO vehicle control was added to the wells. Cells were then incubated at 37 ^{o}C for 1, 2, and 3 days. Cell viability was determined using the Promega Cell Titer 96 Aqueous One Solution cell proliferation assay. Absorbance at 490 nm was read on Tecan Infinite F200 Pro plate reader, and values were expressed as percent of absorbance from cells incubated in DMSO alone.

4.3.3. Western blot

Cells were seeded in 100 mm culture dishes (1×10^6 cells/dish), and allowed to attach overnight. Compound **19** was added at the concentrations indicated compound (0.05, 0.1, 0.5, 1, and 2 μM) and the cells were incubated for an additional 24 h. For comparison, cells were also incubated with DMSO (1%) or geldanamycin (1 μM) for 24 h. Cells were harvested in

ice-cold lysis buffer (23 mM Tris-HCl pH 7.6, 130 mM NaCl, 1% NP-40, 1% sodium deoxycholate, 0.1% SDS), and 30 μg of lysate per lane was separated by SDS-PAGE and followed by transferring to a PVDF membrane (Bio-Rad). The membrane was blocked with 5% skim milk in TBST, and then incubated with the corresponding antibody (EGFR, Her2, Met, Akt, c-Raf, Hsp90, Hsp70, PARP, caspase3, cleaved caspase3, cleaved caspase8, Bcl-2, Bax or β-actin). After binding of an appropriate secondary antibody coupled to horseradish peroxidase, proteins were visualized by ECL chemiluminescence according to the instructions of the manufacturer (GE healthcare, USA).

4.3.4. Apoptosis assay

Cells were seeded in 12-well plates (1×10^5 cells/well), and allowed to attach overnight. Compound **19** was added at the indicated concentration (0.5 and 1 μM) and the cells were incubated for an additional 24 h. After suspended in annexin V binding buffer, cells were stained with annexin V for 15 min and then added to fluorescence-activated cell sorting (FACS) buffer and propidium iodide. Apoptotic cells were measured using BD FACSVerse a flow cytometer.

4.3.5. Protein purification

Recombinant Hsp90 were expressed in *Escherichia coli* BL21 (DE3) cells from pET-15b plasmids. A fresh colony was grown in LB broth medium supplemented with 2.5 mg/mL (500 μL/200 mL) ampicillin at 37 ^{o}C with shacking at 180 rpm until A_{600} reached to about 0.5 and protein expression was induced by the addition of isopropyl-1-thio-β-D-galatopyranoside (final concentration of 1 mM). The temperature was decreased to 18 ^{o}C, and the cell culture was allowed to shake overnight. Cells were harvested by centrifugation (4000 rpm, 20 min, 4

^{o}C). Cell pellets was suspended in binding buffer (20 mM Tris pH 8.0 and 0.5 M NaCl) and sonicated on ice, and clarified by centrifugation at 14000 rpm, 99 min, 4 ^{o}C). His-tagged proteins were purified by nickel-nitriloacetic acid with His Trap column and separated by FPLC using elution buffer (20 mM Tris pH 8.0, 0.5 M NaCl, 1 M imidazole). To verify the purity of Hsp90 protein, the protein was analyzed by SDS-PAGE. Purified proteins were desalted using PD10 column, concentrated in Vivaspin 20 to 2.4 mg/mL, and stored at -70 ^{o}C.

4.3.6. Fluorescence polarization assay

All fluorescence polarization (FP) experiments were conducted in 96-well, black, round-bottom plates using a micro plate reader. For FP assay experiments, to each well was added HFB buffer (20 mM HEPES pH 7.3, 50 mM KCl, 5 mM $MgCl_2$, 20 mM Na_2MoO_4, 0.01% NP-40), 30 nM recombinant Hsp90α full length protein, 5 nM the fluorescein isothiocyanate labeled geldanamycin (GA-FITC) inhibitor, 0.1 mg/mL Bovine globulin (BGG), 2 mM 1,4-dithiothreitol (DTT) and various concentrations of compounds. All wells had a final volume of 100 μL in the HFB buffer. The plate was allowed to be incubated at 4 ^{o}C for 14 h. The polarization values in millipolarization units (mP) were measured at an excitation wavelength at 495 nm and an emission wavelength at 530 nm.

4.3.7. Cytochrome P450 inhibition assay

The inhibitory potency of compound **19** was determined with cytochrome P450 assays in the absence and presence of compound **19** (final concentrations of 0~50 μM with acetonitrile concentration less than 0.5%) using pooled human liver microsomes (Xenotech H0630). All experiments were performed in duplicate. Phenacetin *O*-deethylase, tolbutamide 4-hydroxylase, omeprazole hydroxylase, dextromethorphan *O*-demethylase, and midazolam 1′-hydroxylase activities were determined as probe activities for CYP1A2, CYP2C9, CYP2C19,

CYP2D6, and CYP3A, respectively, using cocktail incubation and tandem mass spectrometry, as described previously.[26]

4.3.8. In vivo xenograft

Eight-week-old female NOD-scid IL2Rgamma^{null} (NSG) mice were purchased from Jackson Laboratory (USA) and maintained in accordance with the institutional guidelines of Keimyung University, College of Medicine. All animal studies were carried out according to approved experimental protocols. The mice were held in individually ventilated cages (IVC) under sterile and standardized environmental conditions (25±2 °C room temperature, 50±10% relative humidity, 12 h light-dark rhythm). H1975 cells (2.0 × 10^6 cells) from an *in vitro* passage were transplanted subcutaneously (s.c.) into the left flank region of mice on day zero. Mice were randomly distributed to the experimental groups (8 mice per group). When the tumors were grown to 500 mm^3 in size, treatment was initiated. Mice were treated intraperitoneally with either compound **19** (10 mg/kg), or DMSO (15 mg/kg) daily followed by weekend rest for 2 weeks. Tumor size was measured at the time of injection and twice per week afterwards with a caliper in two dimensions. Individual tumor volumes (V) were calculated by the formula V= (length × $[width]^2$)/2.

4.3.9. Immunohistochemistry (IHC)

Mouse tissue was fixed with 10% formalin and embedded in paraffin, and sectioned. The sections were stained with IHC for light microscopic examination. For assessment of Akt staining, 5 μm sections were permeabilized in PBS, incubated in 10 mM sodium citrate buffer with pH 6.0 for 100 °C, 10 min, and the with goat polyclonal anti-Akt (Cat #9272, Cell signaling, USA) antibody. Sections were then incubated with secondary antibody (1:200 dilution, Santa Cruz Biotechnology, USA), followed by staining with diaminobenzidine

chromogen (Cat# SK-4105, Vector Laboratories, USA) and counterstaining with hematoxylin (Cat# S3309, Dako, Denmark). The stained sections were examined under microscopy (200) and all histological assessments (Nikon, Japan) were made by a pathologist.

Acknowledgments

This research was supported by Basic Science Research Program through the National Research Foundation of Korea (NRF) funded by the Ministry of Education (NRF-2016R1A6A1A03011325 and 2016R1D1A1B01009559) and by the National Research Foundation of Korea (NRF) grant funded by the Korean Government (MSIP) (No.2014R1A5A2010008).

Appendix A. Supplementary data

References

[1] D. Mahalingam, R. Swords, J.S. Carew, S.T. Nawrocki, K. Bhalla, F.J. Giles, Targeting HSP90 for cancer therapy, British journal of cancer, 100 (2009) 1523-1529.

[2] D. Hanahan, R.A. Weinberg, Hallmarks of cancer: the next generation, Cell, 144 (2011) 646-674.

[3] L. Whitesell, S.L. Lindquist, HSP90 and the chaperoning of cancer, Nature reviews. Cancer, 5 (2005) 761-772.

[4] G. Chiosis, L. Neckers, Tumor selectivity of Hsp90 inhibitors: the explanation remains elusive, ACS chemical biology, 1 (2006) 279-284.

[5] D.B. Solit, G. Chiosis, Development and application of Hsp90 inhibitors, Drug discovery today, 13 (2008) 38-43.

[6] Y.H. Seo, Organelle-specific Hsp90 inhibitors, Arch Pharm Res, 38 (2015) 1582-1590.

[7] A.S. Sreedhar, E. Kalmar, P. Csermely, Y.F. Shen, Hsp90 isoforms: functions, expression and clinical importance, FEBS letters, 562 (2004) 11-15.

[8] D. Chen, A. Shen, J. Li, F. Shi, W. Chen, J. Ren, H. Liu, Y. Xu, X. Wang, X. Yang, Y. Sun, M. Yang, J. He, Y. Wang, L. Zhang, M. Huang, M. Geng, B. Xiong, J. Shen, Discovery of potent N-(isoxazol-5-yl)amides as HSP90 inhibitors, Eur J Med Chem, 87 (2014) 765-781.

[9] Z. Li, L. Jia, J. Wang, X. Wu, H. Hao, Y. Wu, H. Xu, Z. Wang, G. Shi, C. Lu, Y. Shen, Discovery of diamine-linked 17-aroylamido-17-demethoxygeldanamycins as potent Hsp90 inhibitors, Eur J Med Chem, 87 (2014) 346-363.

[10] Z. Li, L. Jia, J. Wang, X. Wu, H. Hao, H. Xu, Y. Wu, G. Shi, C. Lu, Y. Shen, Design, synthesis and biological evaluation of 17-arylmethylamine-17-demethoxygeldanamycin derivatives as potent Hsp90 inhibitors, Eur J Med Chem, 85 (2014) 359-370.

[11] H. Zhao, G. Garg, J. Zhao, E. Moroni, A. Girgis, L.S. Franco, S. Singh, G. Colombo, B.S. Blagg, Design, synthesis and biological evaluation of biphenylamide derivatives as Hsp90 C-terminal inhibitors, Eur J Med Chem, 89 (2015) 442-466.

[12] L. Whitesell, E.G. Mimnaugh, B. De Costa, C.E. Myers, L.M. Neckers, Inhibition of heat shock protein HSP90-pp60v-src heteroprotein complex formation by benzoquinone ansamycins: essential role for stress proteins in oncogenic transformation, Proc Natl Acad Sci U S A, 91 (1994) 8324-8328.

[13] J. Trepel, M. Mollapour, G. Giaccone, L. Neckers, Targeting the dynamic HSP90 complex in cancer, Nature reviews. Cancer, 10 (2010) 537-549.

[14] J.G. Supko, R.L. Hickman, M.R. Grever, L. Malspeis, Preclinical pharmacologic evaluation of geldanamycin as an antitumor agent, Cancer Chemother Pharmacol, 36 (1995) 305-315.

[15] Y. Samuni, H. Ishii, F. Hyodo, U. Samuni, M.C. Krishna, S. Goldstein, J.B. Mitchell, Reactive oxygen species mediate hepatotoxicity induced by the Hsp90 inhibitor geldanamycin and its analogs, Free Radic Biol Med, 48 (2010) 1559-1563.

[16] E. Caldas-Lopes, L. Cerchietti, J.H. Ahn, C.C. Clement, A.I. Robles, A. Rodina, K. Moulick, T. Taldone, A. Gozman, Y. Guo, N. Wu, E. de Stanchina, J. White, S.S. Gross, Y. Ma, L. Varticovski, A. Melnick, G. Chiosis, Hsp90 inhibitor PU-H71, a multimodal inhibitor of malignancy, induces complete responses in triple-negative breast cancer models, Proc Natl Acad Sci U S A, 106 (2009) 8368-8373.

[17] K. Lundgren, H. Zhang, J. Brekken, N. Huser, R.E. Powell, N. Timple, D.J. Busch, L. Neely, J.L. Sensintaffar, Y.C. Yang, A. McKenzie, J. Friedman, R. Scannevin, A. Kamal, K. Hong, S.R. Kasibhatla, M.F. Boehm, F.J. Burrows, BIIB021, an orally available, fully synthetic small-molecule inhibitor of the heat shock protein Hsp90, Mol Cancer Ther, 8 (2009) 921-929.

[18] R. Bao, C.J. Lai, D.G. Wang, H. Qu, L. Yin, B. Zifcak, X. Tao, J. Wang, R. Atoyan, M. Samson, J. Forrester, G.X. Xu, S. DellaRocca, M. Borek, H.X. Zhai, X. Cai, C. Qian, Targeting heat shock protein 90 with CUDC-305 overcomes erlotinib resistance in non-small cell lung cancer, Mol Cancer Ther, 8 (2009) 3296-3306.

[19] S.A. Eccles, A. Massey, F.I. Raynaud, S.Y. Sharp, G. Box, M. Valenti, L. Patterson, A. de Haven Brandon, S. Gowan, F. Boxall, W. Aherne, M. Rowlands, A. Hayes, V. Martins, F. Urban, K. Boxall, C. Prodromou, L. Pearl, K. James, T.P. Matthews, K.M. Cheung, A. Kalusa, K. Jones, E. McDonald, X. Barril, P.A. Brough, J.E. Cansfield, B. Dymock, M.J. Drysdale, H. Finch, R. Howes, R.E. Hubbard, A. Surgenor, P. Webb, M. Wood, L. Wright, P. Workman, NVP-AUY922: a novel heat shock protein 90 inhibitor active against xenograft tumor growth, angiogenesis, and metastasis, Cancer Res, 68 (2008) 2850-2860.

[20] T. Nakashima, T. Ishii, H. Tagaya, T. Seike, H. Nakagawa, Y. Kanda, S. Akinaga, S. Soga,

Y. Shiotsu, New molecular and biological mechanism of antitumor activities of KW-2478, a novel nonansamycin heat shock protein 90 inhibitor, in multiple myeloma cells, Clin Cancer Res, 16 (2010) 2792-2802.

[21] A.J. Woodhead, H. Angove, M.G. Carr, G. Chessari, M. Congreve, J.E. Coyle, J. Cosme, B. Graham, P.J. Day, R. Downham, L. Fazal, R. Feltell, E. Figueroa, M. Frederickson, J. Lewis, R. McMenamin, C.W. Murray, M.A. O'Brien, L. Parra, S. Patel, T. Phillips, D.C. Rees, S. Rich, D.M. Smith, G. Trewartha, M. Vinkovic, B. Williams, A.J. Woolford, Discovery of (2,4-dihydroxy-5-isopropylphenyl)-[5-(4-methylpiperazin-1-ylmethyl)-1,3-dihydrois oindol-2-yl]methanone (AT13387), a novel inhibitor of the molecular chaperone Hsp90 by fragment based drug design, J Med Chem, 53 (2010) 5956-5969.

[22] Y. Wang, J.B. Trepel, L.M. Neckers, G. Giaccone, STA-9090, a small-molecule Hsp90 inhibitor for the potential treatment of cancer, Curr Opin Investig Drugs, 11 (2010) 1466-1476.

[23] K. Jhaveri, T. Taldone, S. Modi, G. Chiosis, Advances in the clinical development of heat shock protein 90 (Hsp90) inhibitors in cancers, Biochim Biophys Acta, 1823 (2012) 742-755.

[24] K. Schunemann, D.P. Furkert, E.C. Choi, S. Connelly, J.D. Fraser, J. Sperry, M.A. Brimble, Synthesis of the 2-methylene analogue of the HRV 3C protease inhibitor thysanone (2-carbathysanone), Org Biomol Chem, 12 (2014) 905-912.

[25] C.H. Jeong, H.B. Park, W.J. Jang, S.H. Jung, Y.H. Seo, Discovery of hybrid Hsp90 inhibitors and their anti-neoplastic effects against gefitinib-resistant non-small cell lung cancer (NSCLC), Bioorg Med Chem Lett, 24 (2014) 224-227.

[26] M.J. Kim, H. Kim, I.J. Cha, J.S. Park, J.H. Shon, K.H. Liu, J.G. Shin, High-throughput screening of inhibitory potential of nine cytochrome P450 enzymes in vitro using liquid chromatography/tandem mass spectrometry, Rapid Commun Mass Spectrom, 19 (2005)

2651-2658.

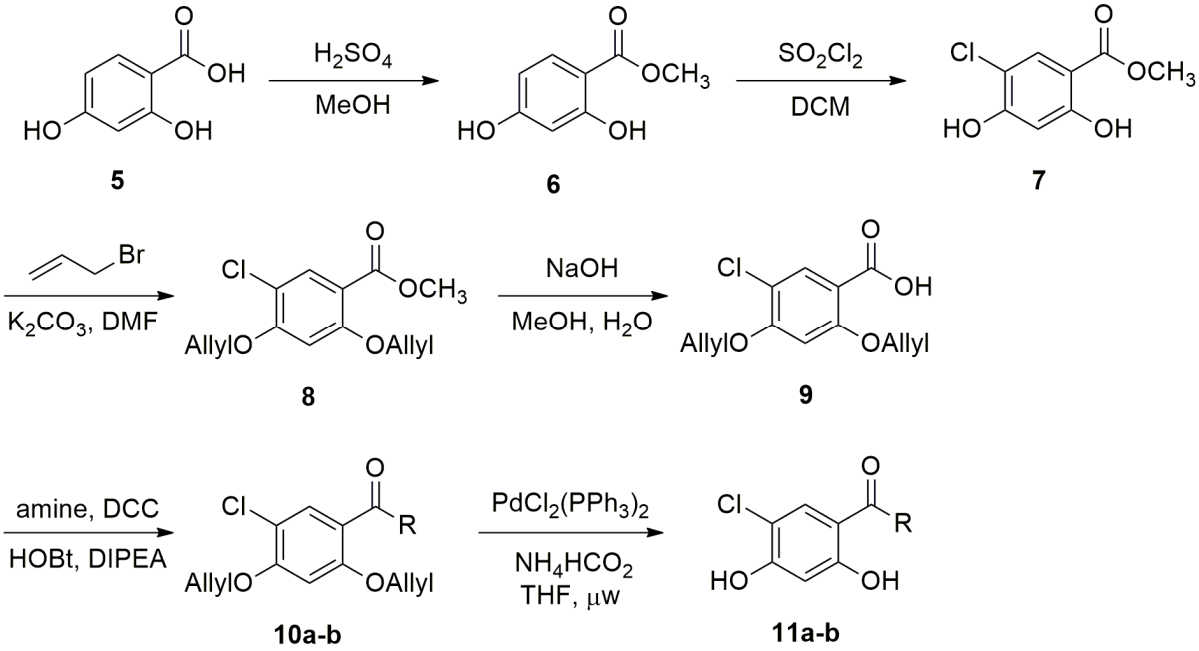

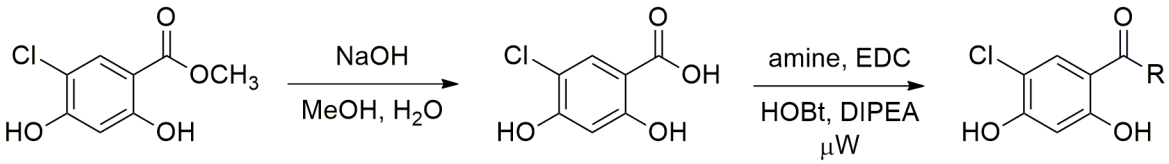

7 **12** **11c-e**